Synthesis and Characterization of Anthra[2,3-*b*]thiophene and Tetraceno[2,3-*b*]thiophenes for Organic Field-Effect Transistor Applications

Famil Valiyev,[†] Wei-Shan Hu,[‡] Hsing-Yin Chen,[†,§] Ming-Yu Kuo,[†] Ito Chao,*[,†] and Yu-Tai Tao*[,†,‡]

Institute of Chemistry, Academia Sinica, Taipei, Taiwan, Republic of China, and Department of Chemistry, National Tsing-Hua University, Hsin-Chu, Taiwan, Republic of China

Received February 18, 2007. Revised Manuscript Received March 29, 2007

A series of thiophene-fused acenes, anthra[2,3-*b*]thiophene (**1**), tetraceno[2,3-*b*]thiophene (**2**), and 2-*n*-decyl-tetraceno[2,3-*b*]thiophene (**3**), were synthesized. The crystal structures of **1** and **2** were determined. A weak dipole results from the addition of the thiophene ring, and the crystal packing changes from the triclinic structure of acenes to orthorhombic, with the molecules maintaining the herringbone arrangement with the molecular long axis antiparallel to the neighbors. Theoretical calculation showed that the molecules have higher oxidation potential and comparable hole mobility as acene analogues with the same number of rings. Thin film transistor devices were fabricated from these materials. With compound **1**, a field-effect mobility of 0.134 cm^2/V s and on/off ratio of 10^8 can be achieved when deposited at a substrate temperature of 25 °C, whereas a mobility of 0.245 cm^2/V s and on/off ratio of 10^6 were observed for compound **2** deposited at 80 °C.

Introduction

Organic field-effect transistors (OFETs) have attracted much attention as low-cost alternatives to conventional silicon-based transistors.[1−3] The most important properties for the active organic materials that comprise the semiconducting layer in an OFET are high mobility, large on/off ratio, stability, and processability. Due to the intensive research efforts in recent years, these attributes have been realized to some extent, particularly in p-channel (hole-transporting) materials, as exemplified by a group of linear, conjugated molecules including oligothiophenes[4−7] and acenes.[8−10] Among these, pentacene is of particularly interest because of its high mobility and high on/off ratio. Many efforts have been devoted to synthesizing pentacene-related derivatives, mainly with substituents at different positions.[9,10] A successful example is the triisopropylsilylethynyl-substituted pentacene, which gave enhanced π-stacking interaction. However, more often than not, the substitution greatly perturbed the crystal packing, and gave an unpredictable effect on the intermolecular electronic coupling, which is highly sensitive to the relative disposition of neighboring molecules. A closely related material with a minor change of the long, platelike molecular shape of pentacene and the packing thereof would be an acene fused with heteroaromatics such as thiophene units[11] or fused heteroaromatics.[12] Anthracene fused with a thiophene unit at both ends has been reported.[11] Yet the compound was obtained as motif mixtures of *syn* and *anti* isomers that are not easily separable. An acene fused with a thiophene unit at one end becomes unsymmetrical and is expected to have nearly the same molecular shape associated with a small dipole moment, which may enhance the intermolecular packing without major change in the molecular arrangement in the crystal, or, preferably, induce a more favorable cofacial π-stacking structure.[13] In this paper, we introduce a new synthetic methodology which avoids the commonly used mercury

* Corresponding author. E-mail: ytt@chem.sinica.edu.tw. Phone:+886-2-27898580.
† Academia Sinica.
‡ National Tsing-Hua University.
§ Current address: Faculty of Medicinal and Applied Chemistry, Kaohsiung Medical University, Kaohsiung, 807 (Taiwan).

(1) Horowitz, G. *Adv. Mater.* **1998**, *10*, 365.
(2) Sun, Y.; Liu, Y.; Zhu, D. *J. Mater. Chem.* **2005**, *15*, 53.
(3) Dimitrakopoulos, C. D.; Malenfant, P. R. L. *Adv. Mater.* **2002**, *14*, 99.
(4) Horowitz, G.; Fichou, D.; Peng, X. Z.; Xu, Z. G.; Garnier, F. *Solid State Commun.* **1989**, *72*, 381.
(5) Servet, B.; Horowitz, G.; Ries, S.; Lagorsse, O.; Alnot, P.; Yassar, A.; Deloffre, F.; Srivastava, P.; Hajlaoui, R.; Lang, P.; Garnier, F. *Chem. Mater.* **1994**, *6*, 1809.
(6) Garnier, F.; Yassar, A.; Hajlaoui, R.; Horowitz, G.; Deloffre, F.; Servet, B.; Ries, S.; Alnot, P. *J. Am. Chem. Soc.* **1993**, *115*, 8716.
(7) Akimichi, H.; Waragai, K.; Hotta, S.; Kano, H.; Sakati, H. *Appl. Phys. Lett.* **1991**, *58*, 1500.
(8) Gundlach, D. J.; Lin, Y.-Y.; Jackson, T. N. *IEEE Electron. Device Lett.* **1997**, *18*, 87.
(9) (a) Meng, H.; Bendikov, M.; Mitchell, G.; Helgeson, R.; Wudl, F.; Bao, Z.; Siegrist, T.; Kloc, C.; Chen, C. H. *Adv. Mater.* **2003**, *15*, 1090. (b) Klauk, H.; Halik, M.; Zschieschang, U.; Schmid, G.; Radlik, W.; Weber, W. J. *J. Appl. Phys.*, **2002**, *92*, 5259. (c) Sakamoto, Y.; Suzuki, T.; Kobayashi, M.; Gao, Y.; Fukai, Y.; Inoue, Y.; Sato, F.; Tokito, S. *J. Am. Chem. Soc.* **2004**, *126*, 8138.
(10) (a) Anthony, J. E. *Chem. Rev.* **2006**, *106*, 5028. (b) Anthony, J. E.; Brooks, J. S.; Eaton, D. L.; Parkin, S. R. *J. Am. Chem. Soc.* **2001**, *123*, 9482. (c) Payne, M. M.; Parkin, S. R.; Anthony, J. E.; Kuo, C.-C.; Jackson, T. N. *J. Am. Chem. Soc.* **2005**, *127*, 4986.
(11) Laquindanum, J. G.; Katz, H. E.; Lovinger, A. J. *J. Am. Chem. Soc.* **1998**, *120*, 664.
(12) Xiao, K.; Liu, Y.; Qi, T.; Zhang, W.; Wang, F.; Gao, J.; Qiu, W.; Ma, Y.; Cui, G.; Chen, S.; Zhan, X.; Yu, G.; Qin, J.; Hu, W.; Zhu, D. *J. Am. Chem. Soc.* **2005**, *127*, 13281.
(13) Bredas, J. L.; Beljonne, D.; Coropceanu, V.; Cornil, J. *Chem. Rev.* **2004**, *104*, 4971.

10.1021/cm070472d CCC: $37.00
Published on Web 05/12/2007

Scheme 1. Synthesis of Compounds 1 and 2[a]

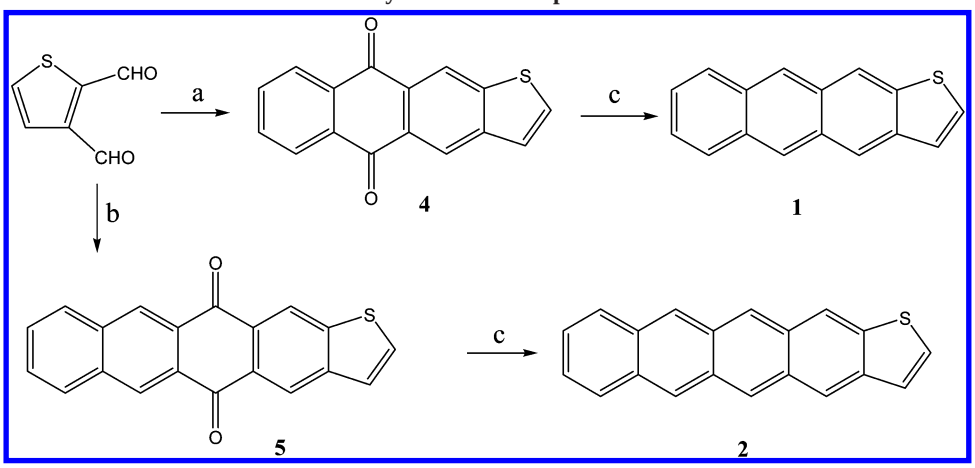

[a] Reagents and conditions: (a) naphthalene-1,4-diol, pyridine, reflux, 6 h, 68%; (b) anthracene-1,4-diol, pyridine, reflux, 6 h, 70%; (c) $LiAlH_4$, THF, 0 °C, 3 h, 85%.

Scheme 2. Synthesis of Compound 3[a]

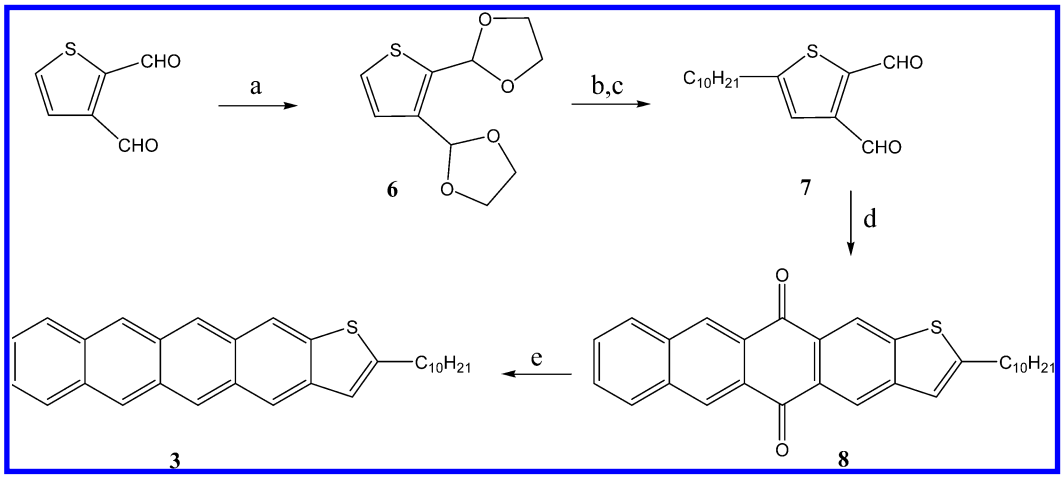

[a] Reagents and conditions: (a) $HOCH_2CH_2OH$, TsOH, benzene, reflux, 12 h, 90%; (b) n-BuLi, $C_{10}H_{21}I$, THF, −78 °C to room temperature, 12 h; (c) THF, HCl, reflux, 15 min, 70%; (d) anthracene-1,4-diol, pyridine, reflux, 6 h, 75%; (e) $LiAlH_4$,THF, 0 °C, 3 h, 85%.

reagent to efficiently prepare several thiophene-fused acene derivatives, anthra[2,3-*b*]thiophene (**1**), tetraceno [2,3-*b*]-thiophene (**2**), and 2-*n*-decyl- tetraceno[2,3-*b*]thiophene (**3**).[14] The single-crystal X-ray structures of **1** and **2** were determined and compared with that of pentacene and tetracene, respectively. Theoretical calculations of the reorganization energy, electronic coupling, and charge mobility were carried out on these compounds and compared with that of pentacene and tetracene. It turns out the crystal packing of **1** and **2** are indeed more compact and changed from the triclinic crystals of acenes to orthorhombic structure, nevertheless maintaining the herringbone-type arrangement of the molecules. However, the calculated electronic coupling and charge mobility are at most similar to that of pentacene, presumably because the slight change in the relative disposition in the crystal reduces the intermolecular electronic coupling. The thin film morphologies, as well as field-effect mobilities, of this series of compounds in a standard thin film transistor configuration are presented.

Experimental Section

Compounds **1**−**3** were synthesized in the laboratory (the synthetic details are provided in Supporting Information) and purified by sublimation. Compound **1**, which is soluble in organic solvents such as chloroform, methylene chloride, THF, and benzene, was characterized by NMR and mass and elemental analyses, whereas compounds **2** and **3** were characterized by mass and elemental analyses. The *n*-octadecyltrichlorosilane(OTS) was purchased from Arcos.

The silicon wafers, with 300 nm thermally grown oxide layer, were cleaned by piranha solution and rinsed thoroughly with ultrahigh purity water. The cleaned silicon wafers were soaked in 1 mM OTS solution in dry toluene for 3 min to generate the OTS-modified silicon oxide surface, designated as OTS−SiO_2/Si. Thin films of **1**, **2,** and **3** were thermally evaporated under a vacuum of 1×10^{-5} Torr and deposited on SiO_2/Si or OTS−SiO_2/Si surfaces at different substrate temperatures. The film thickness was monitored with a quartz crystal microbalance (QCM), and the deposition was controlled at a rate of ∼0.5 Å/s. Atomic force microscopic analyses were carried out by using a Digital Instruments Multimode 3 atomic force microscope. Images were captured by tapping mode with a silicon tip at 300 kHz frequency.

The powder X-ray diffraction was carried out by using the Philips X'Pert diffractometer with X'Celerator detector. The Cu Kα

(14) As this manuscript is being prepared, it is noted that similar work on compounds **1** and **2** was published: Tang, M. L.; Okamoto, T.; Bao, Z. *J. Am. Chem. Soc.* **2006**, *128*, 16002.

Table 1. Lattice Parameters of Pentacene, Tetracene, and Compounds 1 and 2 at 300 K

	pentacene[a]	**2**	tetracene[b]	**1**
a (Å)	6.27	5.92	6.06	5.90
b (Å)	7.78	7.64	7.84	7.68
c (Å)	14.53	29.52	13.01	24.57
α (deg)	76.48	90	77.13	90
β (deg)	87.68	90	72.12	90
γ (deg)	84.68	90	85.79	90
cell density (g/cm^3)	1.35	1.42	1.32	1.40

[a] From ref 17. [b] From ref 18.

Table 2. Dipole Moments, Reorganization Energies of the Hole Transport (λ^+), and Adiabatic Ionization Potentials (IP) Calculated at the B3LYP/6-31G Level[a]**

compound	dimer	dipole (Debye)	λ^+ (meV)	IP (eV)	*R* (Å)	t^+ (meV)	μ^+ (cm^2 V^{-1} s^{-1})
pentacene	D1	0.00	94	5.888	6.27	34	1.93
	D2				4.76	75	5.43
	D3				5.22	44	2.25
2	D1	0.86	97	6.013	5.92	22	0.69
	D2				4.89	51	2.53
	D3				4.93	57	3.21
tetracene	D1	0.00	113	6.270	6.06	16	0.30
	D2				4.77	68	3.39
	D3				5.13	22	0.42
1	D1	0.84	109	6.421	5.90	26	0.81
	D2				4.90	59	2.81
	D3				4.91	61	3.04

[a] The distances between molecular centers (*R*), electronic couplings (t^+) of HOMOs, and hole mobilities (μ^+) of different types of neighboring dimers are also given.

radiation at a power of 45 kV and 40 mA with a scanning step size of 0.008° was used.

FET devices were fabricated with the 300 nm-thick SiO_2 surface as the gate dielectric and the highly n-doped silicon wafer as the gate electrode. The 50 nm-thick gold source and drain electrodes were deposited on the organic films (top contact) through a shadow mask. The channel length (*L*) and width (*W*) are 50 and 500 μm, respectively. The electrical characteristics of the devices were measured in air using a computer-controlled Agilent 4156C semiconductor parameter analyzer. The field-effect mobility of the OFET device was calculated from the saturation region according to eq 1

$$I_{ds,sat} = (WC_i/2L)\mu_{sat}(V_{gs} - V_{th})^2 \quad (1)$$

where *W* and *L* are the channel width and length, respectively, C_i is the capacitance per unit area of the SiO_2 insulator, V_{gs} is the gate voltage, and V_{th} is the threshold voltage.

Results and Discussion

Synthesis. Scheme 1 shows the synthetic route to compounds **1** and **2**. Reaction of commercially available thiophene-2,3-dicarbaldehyde with naphthalene-1,4-diol or anthracene-1,4-diol[15] yielded the quinones **4** or **5** in 70% yield. Reduction of diketones **4** and **5** by the literature procedure of Al-amalgam[16] gave lower yields, along with monoketone and dihydroxy products. Instead, we found that reduction directly with $LiAlH_4$ resulted in ~85% yield of **1** and **2**.

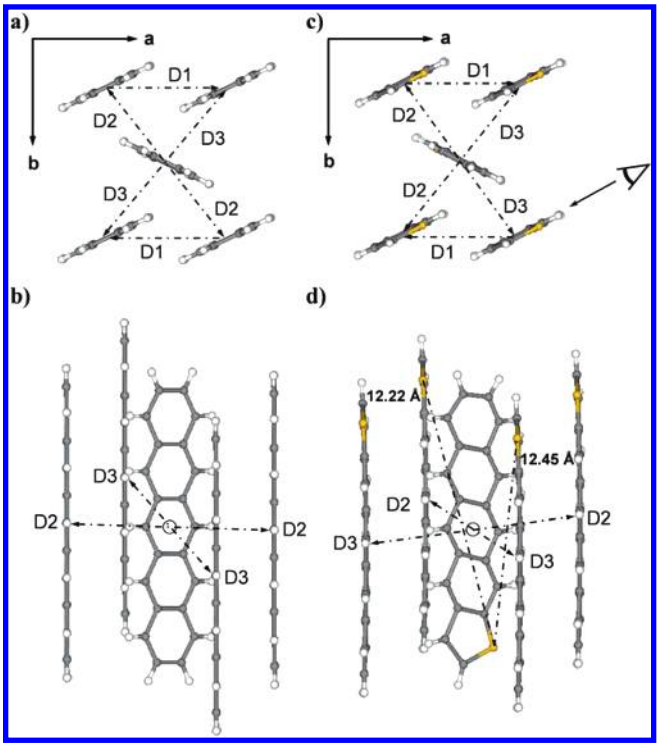

Figure 1. Neighbors of different dimer type (D*n*): (a) pentacene within the *ab* layer of crystal, (b) side view of packing of pentacene, (c) compound **2** within the *ab* layer of crystal, (d) side view of packing of compound **2**.

This approach offers an environmentally benign alternative route to the fused ring system.

2-*n*-Decyl-tetraceno[2,3-*b*]thiophene (**3**) was synthesized according to Scheme 2, which involves the alkylation of a protected dialdehyde. After deprotection, the alkylated dialdehyde was reacted with anthracene-1,4-diol in a manner similar to the synthesis of **1** and **2** to give compound **3** in 64% yield in two steps.

Thermal gravimetric analysis showed that compound **1** exhibited very similar decomposition behavior as tetracene in that 5% weight loss occurred around 280 °C, whereas compound **2** behaved similarly to pentacene, with 5% weight loss occurring above 370 °C. Compound **3** also decomposed near 370 °C.

Crystal Structures and Theoretical Calculation. Single crystals of compounds **1** and **2** were obtained by slow sublimation of the compounds in a temperature-gradient furnace. Single-crystal X-ray analyses revealed the exact packing structures of planar **1** and **2** molecules. The crystal structure of **2** is shown in Figure 1, together with that of pentacene[17] for comparison. The pertinent parameters for the crystals are listed in Table 1. The cell parameters show that the crystal of **2** is more compact than that of pentacene except in the *c*-axis. Introduction of a fused thiophene unit on one end of tetracene moiety generates a small molecular dipole for **2** (ca. 0.85 Debye by calculation, see Table 2) and changes the triclinic $P\bar{1}$ space group of oligoacene into orthorhombic $P2_12_12_1$.[17,18] With the nonzero molecular dipole

(15) Hua, D. H.; Tamura, M.; Huang, X.; Stephany, H. A.; Helfrich, B. A.; Perchellet, E. M.; Sperfslage, B. J.; Perchellet, J. P.; Jiang, S.; Kyle, D. E.; Chiang, P. K. *J. Org. Chem.* **2002**, *67*, 2907.
(16) Lindley, W. A.; MacDowel, D. W. H.; Petersen, J. I. *J. Org. Chem.* **1983**, *48*, 4419.
(17) Mattheus, C. C.; Dros, A. B.; Baas, J.; Meetsma, A.; de Boer, J. L.; Palstra, T. T. M. *Acta Crystallogr., Sect. C: Cryst. Struct. Commun.* **2001**, *57*, 939.
(18) Holmes, D.; Kumaraswamy, S.; Matzger, A. J.; Vollhardt, K. P. C. *Chem. Eur. J.* **1999**, *5*, 3399.

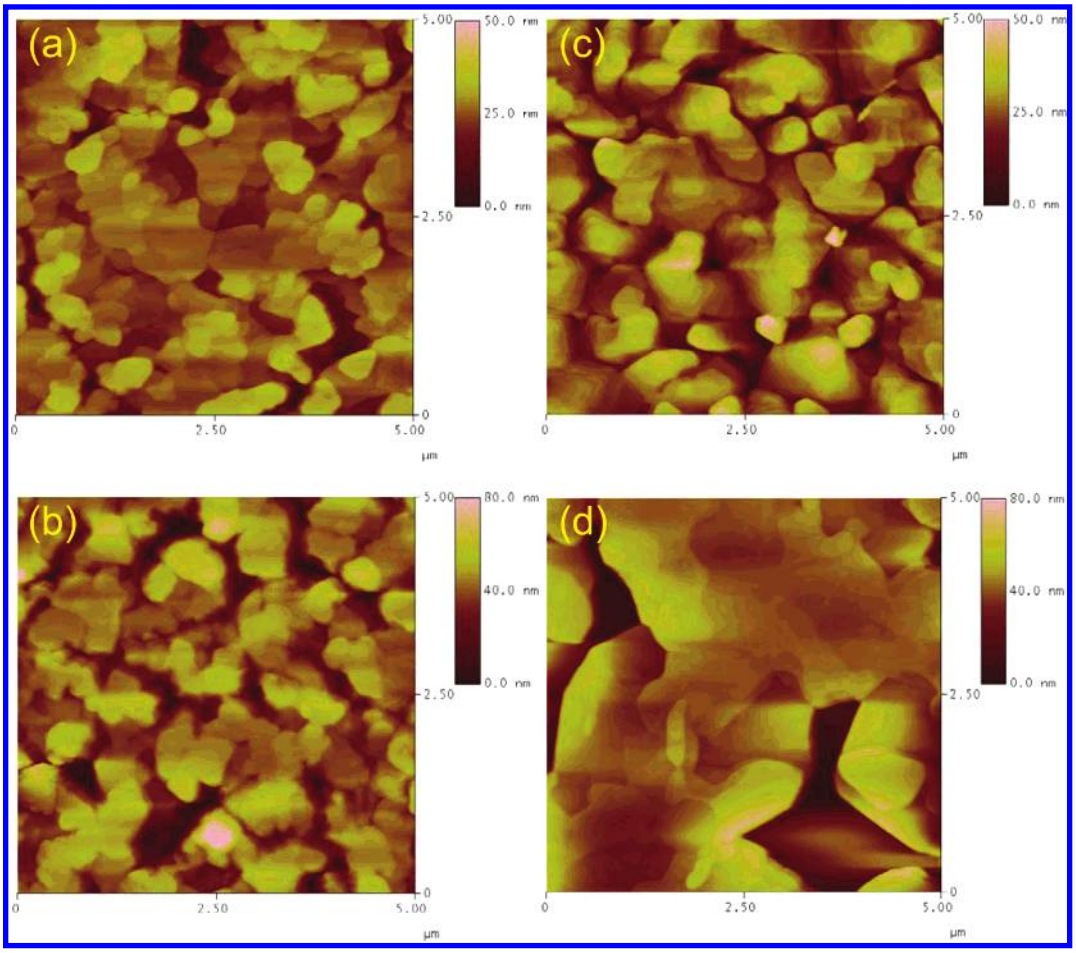

Figure 2. Films of compound **1** on SiO_2 deposited at (a) room temperature and (b) 35 °C, and on OTS−SiO_2 at (c) room temperature and (d) 35 °C

moment, the crystal packing of the thiophene-fused system exhibits antiparallel packing as one might expect, yet there remains a herringbone arrangement of the molecules within the crystal. The distances between molecular centers of **2** along different directions (D1, D2, D3 in Figure 1) were not always shorter than those of pentacene as there are different parallel shifts among the molecules within the unit cell. This will also have an effect on the electronic coupling.[13,19] A similar situation was observed between **1** and tetracene (shown in Supporting Information). Perhaps molecules with a larger dipole moment, and thus stronger intermolecular interactions, are needed to result in smaller packing distances or less shifts. One interesting feature of compound **2** is that equivalent dimer pairs are found along the *b*-axis (see D2 or D3 in Figure 1c), rather than along the $a + b$ direction for D2 and $a - b$ direction for D3 as in pentacene (Figure 1a). Efforts to obtain a single crystal for compound **3** were unsuccessful.

The calculated reorganization energies and electronic couplings based on the molecular and crystal structures are shown in Table 2 (see computational details in Supporting Information).Values of internal reorganization energy for the hole transport (λ^+) of oligoacenes and thiophene-fused oligoacenes were roughly the same when compounds with the same number of rings were compared. Meanwhile, the ionization potentials (IPs) of **1** and **2** were somewhat higher (0.12−0.15 eV) than those of pentacene and tetracene, indicating that these derivatives may be more stable toward oxidation than the corresponding oligoacenes. This has been suggested by the UV absorption experiments.[14] The relative stability was also manifested in the color change of the solution: compound **1** in $CHCl_3$ retained its blue color, whereas the color of tetracene in $CHCl_3$ changed in minutes.

Electronic couplings are strongly dependent on the relative orientations of molecules and thus the specific direction in a crystal. It has been shown for a cofacial dimer of pentacene that the electronic coupling between the highest occupied molecular orbital (HOMO) is oscillatory and progressively reduced when one molecule is shifted along the long molecular axis with fixed $\pi-\pi$ distance.[13,19] The absolute value of electronic coupling is the largest at the perfectly cofacial position where the global overlap between the π orbitals is maximized and reaches zero at the shift of about two-thirds of a ring (ca. 1.7 Å) where the presence of nodal planes causes perfect cancellation of bonding and antibonding overlap between molecules. Although the crystal structures of oligoacenes and the thiophene-fused analogues are herringbone rather than cofacial, similar oscillatory behaviors of the electronic coupling are expected when molecules are shifted along the direction of the molecular axis. Therefore, it is not surprising that the D2 dimer pair of pentacene, which has the smallest shift along the molecular axis (Figure 1b),

(19) Kwon, O.; Coropceanu, V.; Gruhn, N. E.; Durivage, J. C.; Laquindanum, J. G.; Katz, H. G.; Cornil, J.; Brédas, J. L. *J. Chem. Phys.* **2004**, *120*, 8186.

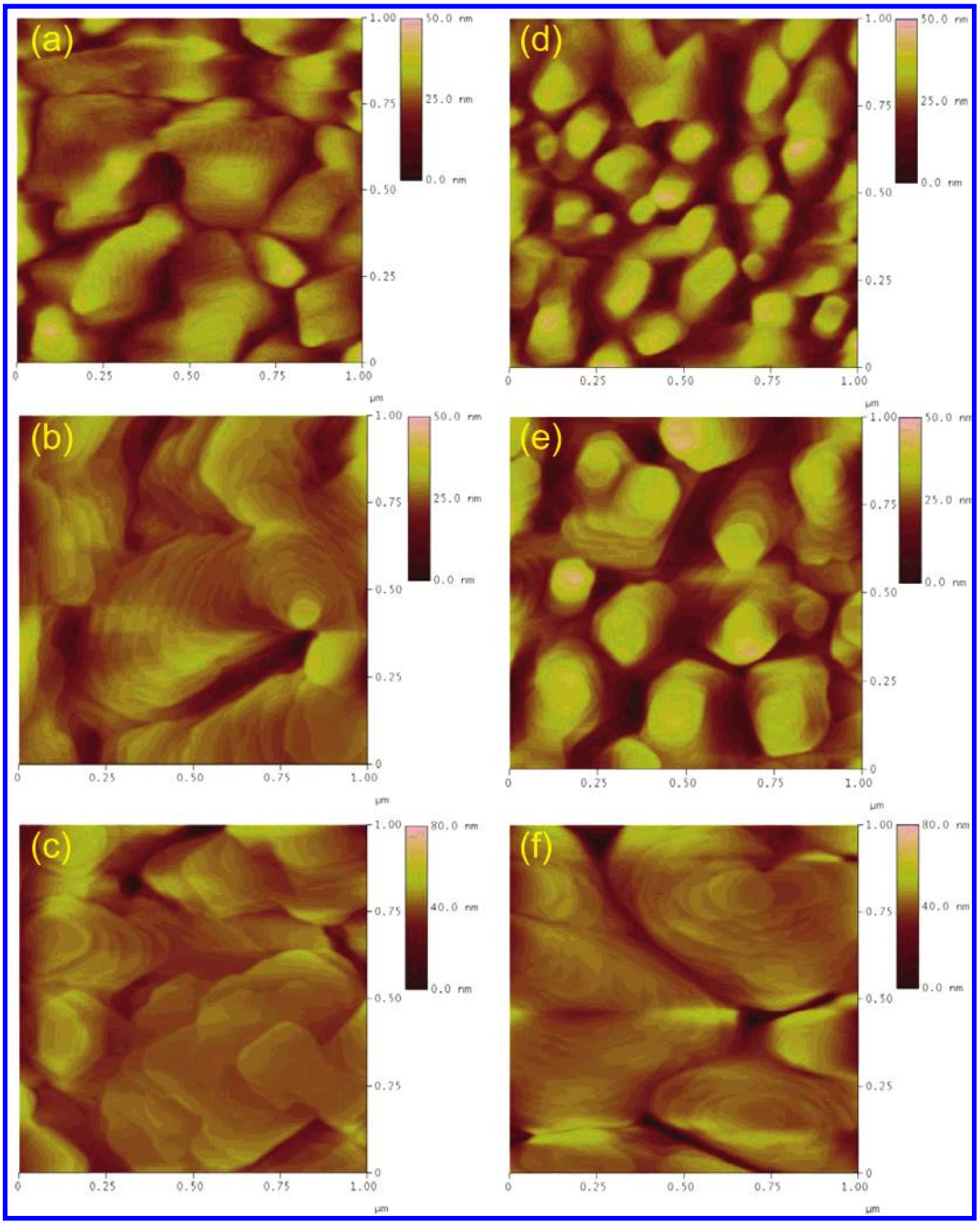

Figure 3. Films of compound **2** deposited on SiO_2 at (a) room temperature, (b) 50 °C, and (c) 80 °C, and on OTS at (d) room temperature, (e) 50 °C (e), and (f) 80 °C (f).

has the largest electronic coupling (75 meV) for the hole transport (t^+) among all t^+ values for pentacene and **2** (Table 2). A similar situation is found for tetracene and **1** because the basic crystal packing features of these compounds are the same as those of their longer analogues.

For a thin-film OFET, it is believed that the hopping mechanism is likely to be responsible for transport of charges. With theoretically calculated λ^+ and t^+, one can calculate the rate of hole transport using Marcus theory.[20] With the rates of hole transport and the known crystal structures, one can then estimate the diffusion coefficients and mobilities of charge carriers. On the basis of this very crude approximation, it is predicted that **2** may be slightly inferior to pentacene (Table 2). It is well-known in the literature that pentacene has better hole-mobility than tetracene does. Our calculated mobilities of pentacene and tetracene are in agreement with this trend, and the phenomenon can be explained by the smaller λ^+ and larger t^+ of pentacene than those of tetracene. Interestingly, although λ^+ values of **2** and **1** follow the rule of extended charge delocalization leading to a small internal reorganization energy,[21] for the antiparallel herringbone structures of this series, the t^+ values of the smaller analogue are in fact slightly larger. Therefore, the calculated mobilities of **2** and **1** closely resemble each other. With similar mobility and yet higher IP, **1** may be preferred

(20) Marcus, R. A. *Rev. Mod. Phys.* **1993**, *65*, 599.

(21) Hutchison, G. R.; Ratner, M. A.; Marks, T. J. *J. Am. Chem. Soc.* **2005**, *127*, 2339.

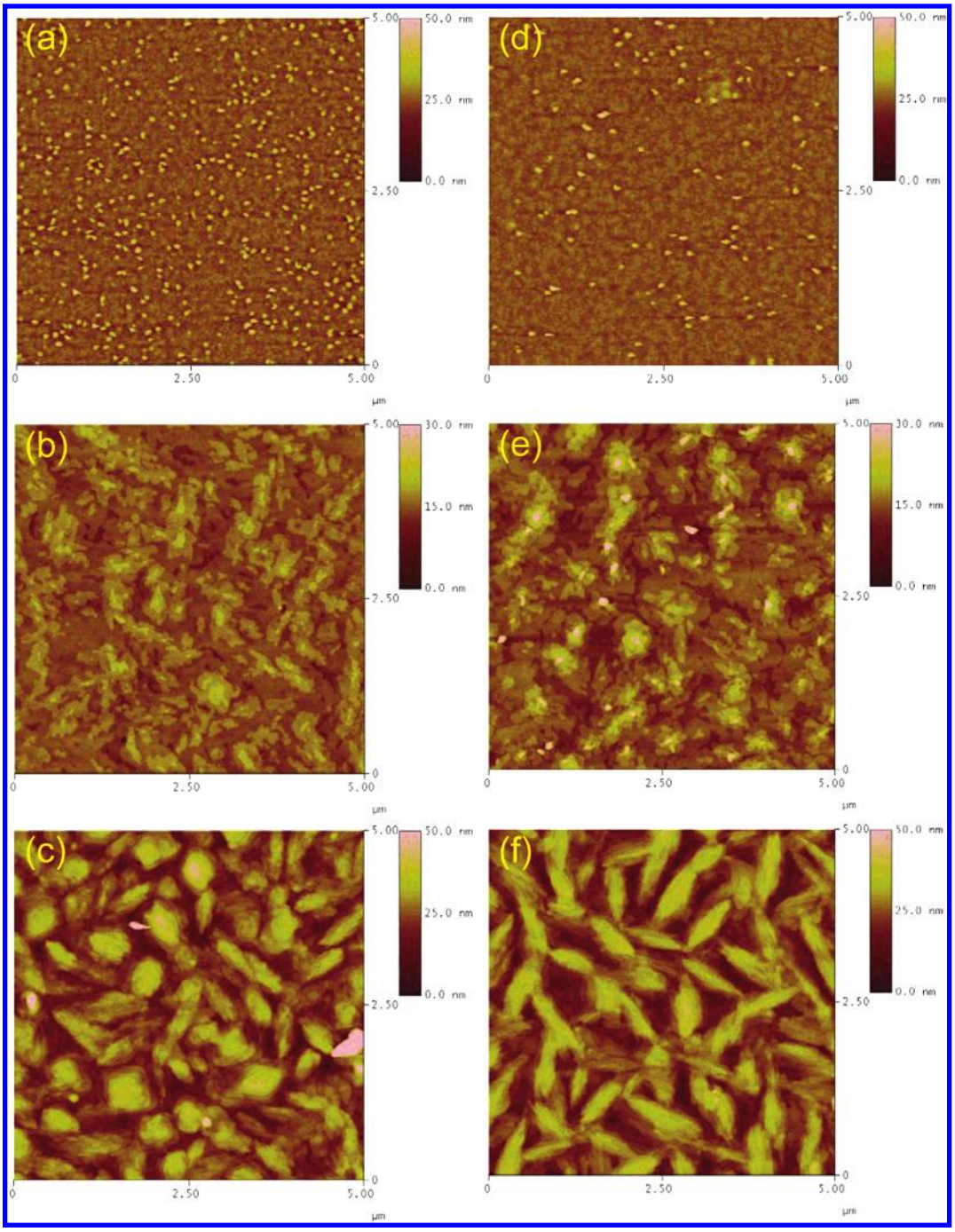

Figure 4. Films of compound **3** deposited on SiO_2 at (a) room temperature, (b) 50 °C, and (c) 80 °C, and on OTS−SiO_2 at (d) room temperature, (e) 50 °C (e), and (f) 80 °C (f).

over **2** under the consideration of both mobility and stability against oxidation.

Thin Film Deposition and Structure Characterization. The AFM images of 50 nm-thick films of compound **1** deposited on SiO_2/Si and OTS−SiO_2/Si surfaces at different temperatures are shown in Figure 2. Several substrate temperatures were used during the deposition process. However, with the substrate temperature higher than 40 °C, the deposited film appeared rather rough, and there was no film deposited when the substrate temperature was higher the 50 °C. Compound **1** deposited on SiO_2/Si at room temperature (25 °C) showed larger terrace structure than that deposited on an OTS−SiO_2/Si surface. At a substrate temperature of 35 °C, the film of compound **1** deposited on SiO_2/Si exhibited a certain degree of melted morphology. On the other hand, the film deposited on OTS−SiO_2 at 35 °C gave significantly larger grains, with the largest grains of 5 μm in Figure 2 of an average dimension. AFM micrographs of films of compound **2** deposited on SiO_2/Si and OTS−SiO_2/Si surfaces at different substrate temperatures are shown in Figure 3. Grains on the SiO_2/Si surface were larger than those deposited on the OTS−SiO_2/Si surface at substrate temperatures of 25 and 50 °C. A similar decreasing trend in grain size was observed for pentacene deposited on SiO_2/Si and OTS−SiO_2/Si surfaces, respectively.[22]

(22) Weng, S. Z.; Hu, W. S.; Kuo, C. H.; Tao, Y. T., Fan, L. J.; Yang, Y. W. *Appl. Phys. Lett.* **2006**, *89*, 172103.

This would imply lower mobility of the molecules on the OTS-covered surface and thus more nucleation sites and smaller grains. However, films of compound **2** deposited on OTS−SiO_2 (as well as on SiO_2) at a substrate temperature of 80 °C gave very large grain size and smooth and clear terrace structure. Films of compound **3** deposited on SiO_2/Si and OTS−SiO_2/Si are distinctly different, as shown in Figure 4. Films deposited at room temperature are smoother yet less crystalline, as also shown by X-ray diffraction (vide infra). The flexible chain attached to the chromophore makes it less readily crystallized at this temperature. Clear and larger terrace packing was found at the deposition temperature of 50 °C. Films deposited at 80 °C show even larger yet discrete and elongated grains, and thus are morphologically rougher. For those analogues without the alkyl chain, **1** and **2**, which form round crystals, the crystal growth is more or less two-dimensional considering the herringbone packing motif. The introduction of the alkyl chain, and thus the packing interaction between chains, increases the growth rate in one direction rather than the other, resulting in long rodlike crystals.

Figure 5 shows the powder X-ray diffraction of films of **1**, **2**, and **3** deposited on SiO_2/Si and OTS−SiO_2/Si at different temperatures. Diffraction peaks at 2θ of 7.22°, 14.41°, 21.67°, and 28.98° are the only peaks obtained for **1** at all substrates at the temperatures used and are assigned as the diffractions from the (001), (002), (003), and (004) planes, respectively. This indicates the same crystalline phase at different deposition conditions. The *d*-spacing calculated from the (001) peak is 12.24 Å, compared to the calculated molecular length of 11.8 Å, suggesting molecules of **1** were standing near upright on SiO_2/Si and OTS−SiO_2/Si surfaces. This orientation will facilitate charge transport in a horizontal device configuration since the direction of $\pi-\pi$ stacking of the herringbone arrangement parallels the conduction path. The peak intensities nevertheless showed different trends, decreased with increasing substrate temperature on the SiO_2/Si surface, and increased with increasing temperature on the OTS−SiO_2/Si surface. Thus, a higher substrate deposition temperature did not necessarily result in a higher quality crystal. Figure 5b shows films of **2** deposited on SiO_2/Si and OTS−SiO_2/Si at different substrate temperatures. Again, a single crystalline phase giving diffraction peaks at 2θ of 5.98° (001), 11.96° (002), 18.01° (003), and 24.06° (004), respectively, was obtained at different substrate temperature. The presence of a single crystalline phase is in contrast with pentacene, which gave a mixture of thin-film phase and bulk phase when deposited on OTS−SiO_2/Si surfaces. The *d*-spacing calculated from (001) is 14.76 Å which also indicates a perpendicular orientation of **2** on the surfaces. In contrast, films of compound **3** gave a single diffraction peak at 2θ of 3.24°. The *d*-spacing calculated from this diffraction peak is 27.24 Å. While the single-crystal data are unavailable for this compound, it is reasonable to assume the packing of the aromatic moieties dominates the crystal packing, which was shown to be antiparallel for compounds **1** and **2**. Assuming the same packing motif of the aromatic moieties, then the number density of the alkyl chains on each side of the packed aromatic layer would be half that of the number

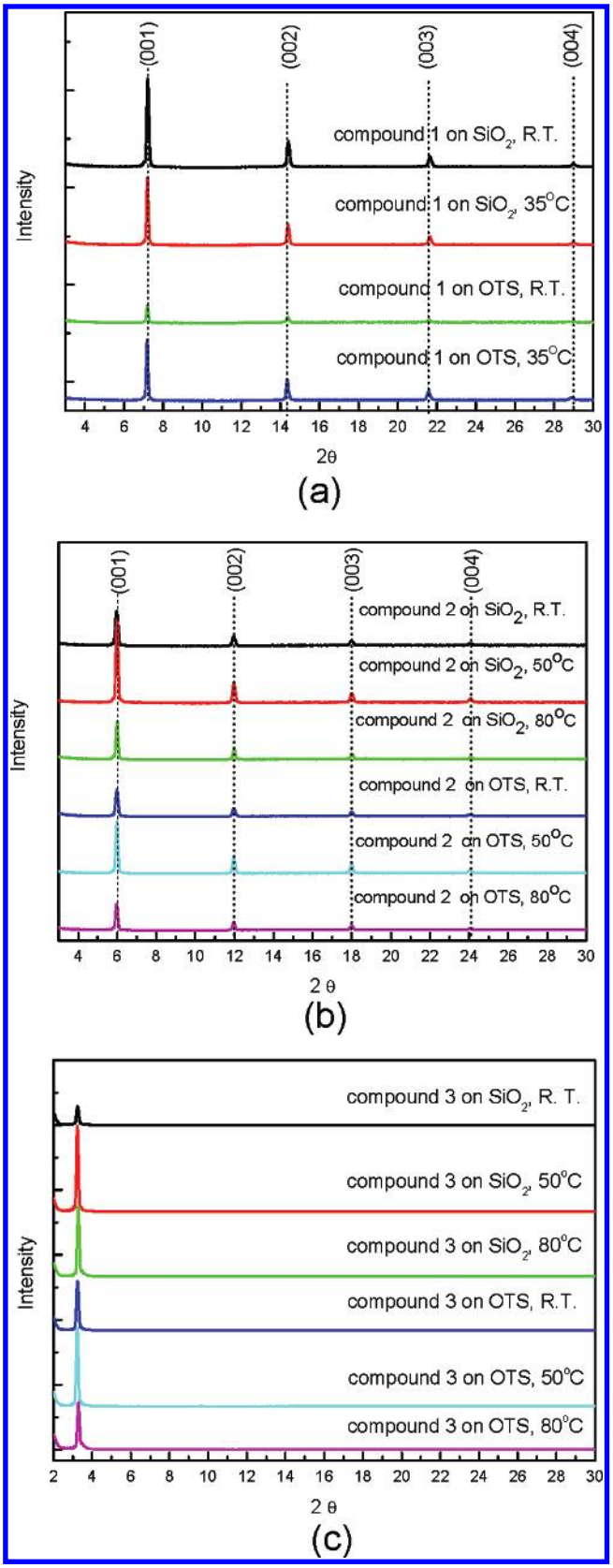

Figure 5. X-ray diffraction of 50 nm-thick film of compounds (a) **1**, (b) **2**, and (c) **3** deposited on SiO_2 and OTS−SiO_2 surfaces at different substrate temperatures.

density of the aromatic moieties. This would cause a substantial tilt of the alkyl chains. A proposed film structure giving a *d*-spacing of 27.24 Å is shown in Figure 6. This structure is similar to that of α,ω-dihexyl-sexithiophene,

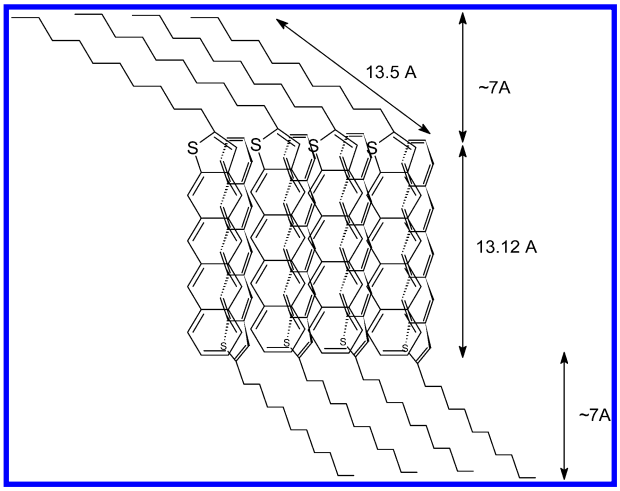

Figure 6. Proposed layer structure of compound **3**.

Table 3. Field-Effect Mobility, On/Off Ratio, and Threshold Voltage for Transistors Fabricated at Different Substrate Temperature and Surfaces

compd **1**	room temp	35 °C
SiO_2	$0.01/10^3$/24 V	$0.004/10^4$/34 V
OTS	$0.134/10^8$/−13 V	$0.004/10^5$/−40 V

compd **2**	room temp	50 °C	80 °C
SiO_2	$0.011/10^3$/26 V	$0.041/10^3$/35 V	$0.008/10^3$/30 V
OTS	$0.037/10^4$/−15 V	$0.104/10^5$/−19 V	$0.245/10^6$/−25 V

compd **3**	room temp	50 °C	80 °C
SiO_2	$0.0013/10^6$/−27 V	$0.0075/10^5$/−2.9 V	$0.008/10^5$/−8.3 V
OTS	$0.0027/10^4$/−0.9 V	$0.05/10^6$/−10.7 V	$0.064/10^6$/−29.5 V

except that the chains tilt more due to the lower number density of alkyl chains. The strongest intensity of the diffraction peak was found when the substrate temperature was kept at 50 °C during the film deposition on SiO_2/Si and OTS−SiO_2/Si surfaces. Further raising substrate temperature resulted in decreasing diffraction intensity. This is in agreement with the AFM observations that the film deposited at 80 °C was noncontinuous and rougher.

FET Device Fabrication and Characterization. Characteristics of FET devices prepared from **1**, **2**, and **3** are shown in Table 3, with the corresponding *I*−*V* curves provided in the Supporting Information. For compound **1**, the best performance was obtained on the OTS−SiO_2/Si surface with a deposition temperature of 25 °C. A mobility of 0.134 cm^2/V s and an on/off ratio up to 10^8 were achieved. Higher deposition temperatures greatly reduced the mobility both on SiO_2/Si and OTS−SiO_2/Si surfaces. From the morphology study by AFM, this may seem surprising, as the crystal size increased with increasing deposition temperature. One possibility is that, at higher substrate temperature, the grains are larger but less connected or poorly contacted. Decreasing mobility with overly increasing grain sizes was also documented in the literature.[23] In comparison with tetracene, a high mobility of 0.1 cm^2/V s can only be obtained for the tetracene molecule on the OTS−SiO_2/Si surface by cooling the substrate to 15 °C, presumably due to the higher volatility of tetracene.[24] Thus, compound **1** offers an advantage over tetracene in terms of mobility and ease of fabrication, and possibly stability. For compound **2,** the best device performance was obtained for film deposited on the OTS−SiO_2/Si surface at a substrate temperature of 80 °C, reaching a mobility of 0.245 cm^2/V s and an on/off ratio of 10^6. These characteristics are comparable to the previous report of 0.31 cm^2/V s obtained at 60 °C.[14] The mobility decreased with lower substrate temperature. This trend parallels that revealed from AFM analyses: the larger the grain size, the higher the mobility. For compound **2** deposited on SiO_2/Si surface, the highest mobility of 0.041 cm^2/V s was obtained at a deposition temperature of 50 °C. Further increasing substrate temperature resulted in reduced grain size and lower device performance. Devices based on compound **3** gave the best performance on the OTS−SiO_2/Si surface at 80 °C, with a mobility of 0.064 cm^2/V s and an on/off ratio of 10^6. Those deposited on SiO_2/Si surfaces are lower, reaching 0.008 cm^2/V s at most.

Chart 1. Fused, Hybrid, Acene−Thiophene-Based Organic Semiconductors

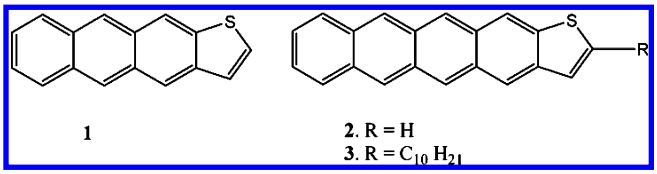

Conclusion

In summary, a series of thiophene-fused oligoacene molecules were synthesized by a route involving $LiAlH_4$-reduction of the diketone as the aromatization step. The thiophene unit imparts a small dipole to the molecules such that the molecules pack antiparallel relative to the neighboring molecules. Yet, the small dipole and minimal change in the molecular shape did not change the herringbone arrangement of the molecules. The reorganization energies for hole transport of the thiophene-fused compounds are similar to those of acene analogues (less than 5% changes), and the calculated electronic couplings based on the single-crystal structures show a similar range as the acene analogues. The deposited films exhibit varied temperature-dependent morphology on different substrates, probably due to complicated sticking efficiency and volatility of the molecules involved. The property of organic semiconducting molecules as channel materials in thin film transistors depends on a number of factors: the reorganization energy, which is intrinsic to the molecular structure; the electronic coupling, which depends on the crystal packing and the relative orientation with respect to the substrate and electrodes; the grain size and morphology, which depend on the nucleation rate and growth rate in different directions. In the current case, the first two factors are similar to those of acene analogues. The third factor is highly sensitive to the deposition condition and harder to compare among different molecules. While the performance of the transistor device was not thoroughly optimized, the mobilities based on the

(23) Laquindanum, J. G.; Katz, H. E.; Lovinger, A. J.; Dodabalapur, A. *Adv. Mater*. **1997**, *9*, 36.

(24) Gundlach, D. J.; Nichols, L.; Zhou, L;, Jackson, T. N. *Appl. Phys. Lett.* **2002**, *80*, 2925.

thiophene-fused acene molecules are similar to those based on corresponding acenes of similar length. With the advantage of better stability and lower volatility relative to the respective acenes, these molecules offer attractive alternatives to the oligoacenes.

Acknowledgment. The authors wish to thank the National Science Council, Taiwan, Republic of China, and Academia Sinica for the financial support. The computing time granted by the National Center for High-Performance Computing and the Computing Center of Academia Sinica is acknowledged.

Supporting Information Available: Experimental, characterization, and computational details; Figures S1−S4 (PDF). This material is available free of charge via the Internet at http://pubs.acs.org.

CM070472D